PFG-NMR Diffusion as a Method To Investigate the Equilibrium Adsorption Dynamics of Surfactants at the Solid/Liquid Interface

Monika Schönhoff* and Olle Söderman

Physical Chemistry 1, Chemical Center, University of Lund, P.O. Box 124, S-22100 Lund, Sweden

Received: April 3, 1997; In Final Form: July 22, 1997[⊗]

The equilibrium dynamics of surfactant exchange between an adsorption layer on polystyrene latex particles and an aqueous solution were investigated for the nonionic poly(ethylene oxide) surfactant $C_{12}(EO)_5$. In this system, surfactant molecules occur in different sites, i.e., in solution and as adsorbed surfactant, where the surfactant in each site exhibits a different diffusion coefficient. NMR diffusion experiments using pulsed field gradients (PFG) and a stimulated echo sequence were performed. On variation of the gradient pulse spacing, Δ, the transition from slow to fast surfactant exchange, as compared to Δ, can be covered, and the region of intermediate exchange is described by a two-site model of exchange-coupled diffusion. Exchange−diffusion experiments on adsorbed surfactant were performed for several surfactant concentrations with varying gradient spacing. Applying a two-site model, we obtained the average residence times of the surfactant in the monolayer and in solution. Error analyses of the fitting procedures were performed by Monte Carlo simulations of the experimental noise. With the PFG-NMR method, adsorption dynamics are studied under equilibrium conditions. We found fast adsorption rates on the order of 10 ms, corresponding to diffusion-controlled adsorption. With increasing surfactant concentration, the dynamics become faster, which we attribute to a large contribution due to exchange between micelles and the surface. PFG-NMR experiments can probe an exchange time scale as fast as milliseconds, which has so far not been achieved for surfactants at solid/liquid interfaces. They might therefore become an interesting tool to investigate equilibrium adsorption dynamics of surfactants beyond the diffusion limit, where the adsorption is kinetically controlled.

Introduction

The adsorption dynamics of surfactant layers at interfaces have mainly been studied by nonequilibrium methods at air/liquid or liquid/liquid interfaces, as for example by the pressure-jump or pendent drop method (see ref 1 and references therein). In most methods, the area of a liquid/gas or liquid/liquid interface is changed stepwise and the time dependence of the surface tension is measured. Such data refer to the nonequilibrium dynamics of the surfactant adsorption, which is mostly governed by diffusion of surfactants to the surface through a surfactant-depleted subsurface layer, described by the theory of diffusion-controlled adsorption.[2,3] Typical time scales for equilibration range from seconds[1] to milliseconds,[4] depending on the geometry of the method.

At solid/liquid interfaces adsorption and desorption dynamics have been studied in nonequilibrium by changing the concentration of the liquid phase.[5] Here, adsorption is again governed by diffusion through a subsurface layer, leading to typical time scales of several hundred seconds for desorption. It would be of interest to study the adsorption dynamics under conditions where the diffusion limitation corresponds to a faster time scale, so that kinetic effects become important and can be studied, e.g., in equilibrium. Theoretical work on kinetic effects has been dealing for example with cohesive energies as kinetic barriers for desorption[6] and electrostatic repulsion between an approaching ionic surfactant molecule and the surface layer as kinetic adsorption barrier.[7]

Here we present the NMR self-diffusion technique as a method to investigate the equilibrium dynamics of surfactants at solid interfaces. Using $C_{12}(EO)_5$, we will show that this technique can, despite the low sensitivity of NMR in general and the low overall surfactant concentration in adsorption samples, probe the equilibrium exchange between a solid surface and bulk solution, provided that appropriate numerical procedures are followed.

The knowledge of some properties of the binary system $C_{12}(EO)_5$/water at low surfactant concentrations is important for the investigation of adsorption layers. Since data for concentrations around and slightly above cmc are not available from the literature, we will first characterize this system with respect to transverse relaxation times and diffusion coefficients of micelles and monomers.

Materials and Methods

Surfactant-free polystyrene latex particles with a narrow size distribution and a spherical shape with a radius $R = 101$ nm, dissolved in aqueous solution (H_2O), were purchased from Polysciences Europe. The surfactant used was dodecylpenta(ethylene oxide) ($C_{12}(EO)_5$) obtained from Nikko, Japan. Samples were prepared at a low latex volume fraction of 1.8 vol %, to avoid obstruction effects that otherwise affect the diffusion coefficients. Surfactant concentrations were on the order of full surface coverage, varying from 0.7 to 1.2 mg/mL. All samples were prepared by weight.

The pulsed field gradient method (PFG)[8−10] was applied to measure surfactant self-diffusion. Due to fast transverse relaxation (T_2) of adsorbed surfactants, a stimulated echo sequence had to be used. The echo intensity of the ethylene oxide peak at 3.6 ppm was determined as a function of the gradient strength g, while the gradient pulse duration, δ, was kept constant. For each surfactant concentration four diffusion experiments were performed with gradient spacings Δ varying from 10 to 100 ms. The gradient pulse duration δ was adjusted accordingly, so that each experiment covered the same range of k values, where $k = \gamma^2 g^2 \delta^2 (\Delta - (\delta/3))$ and γ is the gyromagnetic ratio. To improve the quality of the spectra, three

[⊗] Abstract published in *Advance ACS Abstracts,* September 15, 1997.

S1089-5647(97)01161-9 CCC: $14.00

pregradient pulses with a spacing of Δ were applied directly before the stimulated echo sequence. Depending on sample concentrations and delay times, for each data point sampling of up to 1024 scans was necessary, resulting in experiment times of 3−7 h per decay curve. The echo decay in the case of one-component diffusion is given by

$$\varphi(k) = \frac{1}{2}\exp\left(-\frac{T}{T_1} - \frac{2\tau}{T_2}\right)\exp(-kD) \tag{1}$$

where τ is the time between the first and second 90° pulse, T is the time between the second and third 90° pulse in the stimulated echo sequence and T_1 and T_2 are the longitudinal and transverse relaxation time, respectively.

Relaxation times were determined by means of an inversion recovery (T_1) sequence and a Hahn echo pulse sequence with additional gradient pulses for suppression of remaining protons in D_2O (T_2). All experiments were performed on a Bruker DMX 200 spectrometer with a gradient probe providing a maximum gradient strength of 8.8 T/m, except for monomer diffusion, which was measured on a Varian 360 MHz spectrometer applying a Hahn echo with δ-variation and $\Delta = 30$ ms. All experiments were performed at $T = 293$ K, and in all cases the signal of the ethylene oxide protons at 3.6 ppm was evaluated.

Theoretical Considerations

Surfactants in the system under study occur in three different states: in an adsorption layer around the latex particles, in micellar, and in monomeric form. As further discussed below, the exchange between monomeric and micellar surfactant is fast. Therefore we consider two surfactant sites A and B: Site A is constituted by monomeric and micellar surfactant, characterized by an average diffusion coefficient, D_A, and a mean residence time of a surfactant in this site, τ_A. In site B the adsorbed surfactant is described by a mean residence time τ_B in the adsorption layer and a diffusion coefficient D_B, given by the diffusion of the latex particle, which is given by the Stokes equation. The contribution from lateral diffusion of surfactant along the latex surface is negligible, since the maximum displacement of molecules along the surface is small compared to the mean displacement of the whole particle.

A mathematical model describing the effect of two-site exchange on the echo decay in PFG diffusion experiments has been described by Kärger. In the limit of short gradient pulses ($\delta \ll \Delta$) and taking into account that relaxation times might differ in both sites, the echo decay of a Hahn echo becomes[11]

$$\varphi(g) = p_A \exp(-a_A) + p_B + \exp(-a_B) \tag{2}$$

with

$$a_{A,B} = \frac{1}{2}\left\{k(D_A + D_B) + \Delta\left(\frac{1}{T_A} + \frac{1}{T_B} + \frac{1}{\tau_A} + \frac{1}{\tau_B}\right) \mp \sqrt{\left[k(D_A - D_B) + \Delta\left(\frac{1}{T_B} - \frac{1}{T_A} + \frac{1}{\tau_B} - \frac{1}{\tau_A}\right)\right]^2 + \frac{4\Delta^2}{\tau_A\tau_B}}\right\} \tag{3}$$

$$p_B = \frac{1}{a_B - a_A}\left\{\frac{\tau_A}{\tau_A + \tau_B}\left(kD_A + \frac{\Delta}{T_A}\right) + \frac{\tau_B}{\tau_A + \tau_B}\left(kD_B + \frac{\Delta}{T_B}\right) - a_A\right\} \tag{4}$$

$$p_A = 1 - p_B \tag{5}$$

and

$$k = \gamma^2 g^2 \delta^2 \Delta \tag{6}$$

where T_A, T_B are the transverse relaxation times in the two sites, respectively. In the case of the stimulated echo sequence applied here, both longitudinal and transverse relaxation contributes to the echo decay. Therefore T_A and T_B were replaced by

$$\frac{1}{T_{A,B}} = \frac{T/\Delta}{T_{1A,B}} + \frac{2\tau/\Delta}{T_{2A,B}} \tag{7}$$

Equation 7 takes T_1 relaxation during Δ and T_2 relaxation during 2τ into account.

Two extreme cases of eqs 2−4 can be considered: In slow exchange (neglecting relaxation) where τ_A, $\tau_B \gg \Delta$, the equations decouple to

$$\varphi(g) = (1 - p_B)\exp(-kD_A) + p_B \exp(-kD_B)$$

and

$$p_B = \tau_B/(\tau_A + \tau_B) \tag{8}$$

and the experiment probes the individual diffusion coefficients of molecules in both sites. In fast exchange where τ_A, $\tau_B \ll \Delta$, the decay becomes monoexponential with an averaged diffusion coefficient. In the system under study, we found exchange to occur on an intermediate time scale. Therefore eqs 2−4 were fitted by a Levenberg−Marquard algorithm to data sets consisting of four diffusion experiments with different Δ. The individual echo decays were described by different functions, each with appropriate values of Δ, δ, and τ of the corresponding diffusion experiment. A global set of parameters $P_{res} = (D_A, \tau_A, \tau_B, A_i)$, where A_i ($i = 1-4$) are the signal amplitudes, is optimized to fit the whole set of echo decays. $P_{in} = (T_1, T_{2A}, T_{2B}, D_B)$ is the set of fixed input parameters, which have global values as well.

To check the stability of the results with respect to experimental errors in the data points as well as in the input parameters, we performed Monte Carlo simulations of the effect of data noise and errors of input parameters on the resulting parameters. Alper and Gelb[12] described this procedure and showed that it results in confidence intervals for the resulting parameters that are more accurate than those obtained from standard methods, especially in cases with deviations from normal parameter distributions or with strong covariance between parameters, which is the case in the system under investigation. In a first step, a global fit on the original experimental data set is performed, resulting in a parameter set $P_{res}(0)$. Then the noise level of each data set is calculated by the standard deviation of the experimental data from this fit. As a second step, a loop of N fits is performed, where for each fit (a) artificial noise with the corresponding standard deviation is added to each experimental data set, and (b) the input parameters P_{in} are statistically varied within their error interval, before the global fit is performed on these modified data. The resulting parameter set $P_{res}(n)$ from the global fit is saved. Thus, finally a distribution of resulting parameters $P_{res}(n)$, $n = 1, ..., N$, is obtained. As a third step, the average values, standard deviations, and correlation coefficients of the resulting parameters are calculated.

Results and Discussion

1. Characterization of the Binary System $C_{12}(EO)_5$/Water at Low Concentrations. For a characterization of the surfactant/latex/water system in terms of the model described above,

TABLE 1: T_2 Relaxation of $C_{12}(EO)_5$ in D_2O

c (mg/mL)	slow T_2 (ms)	fast T_2 (ms)
0.0250	380	
0.1203	361	47
0.1817	334	50
0.3578	315	45
0.9766	302	44
10.0969	276	51

the relaxation and diffusion properties of the excess surfactant in water are required. We will therefore first discuss the results for $C_{12}(EO)_5$ in aqueous solution at concentrations around cmc to obtain the parameters T_1, T_{2A}, and the diffusion coefficient of the surfactant in solution. The cmc value of $C_{12}(EO)_5$ in H_2O is 0.026 mg/mL at 20 °C.[13] Additionally we determined the cmc of $C_{12}(EO)_5$ in D_2O at 20 °C by chemical shift changes due to micellization and found a value of 0.0265 ± 0.003 mg/g.

The longitudinal relaxation time T_1 was measured for $C_{12}(EO)_5$ in D_2O at $c = 0.36$ and 0.98 mg/mL, where $T_1 = 465$ ms, independent of concentration. In the T_2 experiments, a double-exponential decay has been observed at concentrations above the cmc. Table 1 gives the relaxation times of the two components as a function of the surfactant concentration. The fast T_2 value is constant, and the intensity ratio of both contributions does not depend on concentration, with the fast component having much lower intensity. Therefore we conclude that the biexponentiality is caused by T_2 varying for different ethylene oxide groups on the same molecule, rather than from different relaxation times of monomers and micelles. The fast component probably arises from the α-EO which is closest to the C_{12} chain and therefore can be more restricted in motion than the other EO groups in the case of aggregated surfactant.

This interpretation is consistent with the assumption of fast exchange between monomers and micelles and is supported by the following arguments: The T_2 relaxation decay for the CH_2 protons in the alkyl chain is monoexponential with $T_2 = 22$ ms (at $c = 10$ mg/mL). As a consequence, slow exchange between different aggregation sites can be excluded as a reason for the occurrence of two components in the relaxation decay of the EO protons. Furthermore, the long T_2 value of the EO protons slightly decreases with increasing concentration. This is inconsistent with this contribution arising from monomers, but can be caused by the α-EO groups in micelles becoming more rigid with increasing concentration, and it thus reflects the increase in micellar size with concentration that has been observed by several authors.[14−16]

Diffusion experiments on binary mixtures of $C_{12}(EO)_5$ in H_2O were done by PFG-NMR measurements with $\Delta = 10$ ms; the other parameters were the same as for the adsorption samples. The decay was monoexponential for all samples, and the results are shown in Figure 1 together with literature data that had been obtained at higher concentrations.

Furthermore, the monomer diffusion coefficient D_1 of $C_{12}(EO)_5$ was measured in D_2O at $c = 0.025$ mg/mL, resulting in a monoexponential echo decay with $D_1 = 3.1 \times 10^{-10}$ m^2/s. Taking the viscosity differences into account, this corresponds to $D_1 = 3.9 \times 10^{-10}$ m^2/s in H_2O, and the resulting hydrodynamic radius is $R_H = 5.5$ Å. We can compare this result to other diffusion measurements so far reported for monomers: For SDS in D_2O at 25 °C it was found that $D_1 = 5 \times 10^{-10}$ m^2/s.[17] $C_{12}(EO)_5$ monomeric diffusion is therefore slightly slower, reflecting the larger size of the headgroup. The diffusion coefficient for $C_{12}(EO)_8$ was determined by radioactive tracer methods at $T = 306$ K in H_2O[18] and results in $R_H = 5.4$ Å, which is very close to the value we obtained for $C_{12}(EO)_5$.

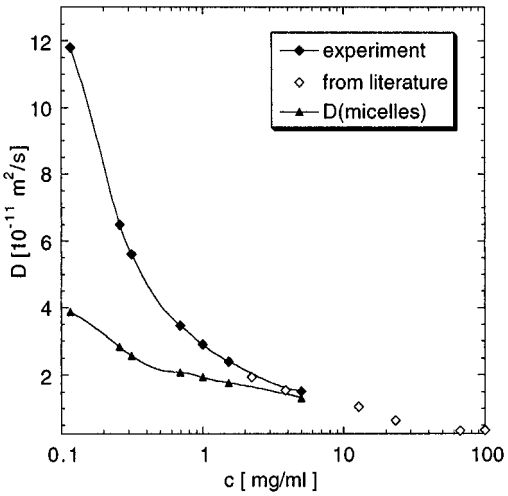

Figure 1. Diffusion coefficient of $C_{12}(EO)_5$ in H_2O. Solid dots: Data from this work. Solid circles: D_{mic}, calculated from eq 9. Open dots: Data from Brown et al.,[16] measured in D_2O at 20.4 °C and recalculated here for $C_{12}(EO)_5$ in H_2O taking into account the difference in solvent viscosity. The solid curves are guidelines for the eye.

As has been discussed previously,[14] at higher concentrations $C_{12}(EO)_5$ appears to form long, rod-shaped micelles with a size that significantly decreases with decreasing concentration, as reflected by the increasing diffusion coefficient. Brown et al. have extrapolated their diffusion data (see Figure 1) to infinite dilution and obtained a hydrodynamic radius of 68 Å.

At even lower concentrations the increase of the diffusion coefficient is due not only to the decrease of micellar size but also to fast exchange with monomers (cf. discussion above), resulting in a contribution from the latter to the observed diffusion coefficient, which in fast exchange between monomers and micelles is described as

$$D = \frac{c - \mathrm{cmc}}{c} D_{\mathrm{mic}} + \frac{\mathrm{cmc}}{c} D_1 \qquad (9)$$

From this equation and using the value of the monomeric diffusion coefficient D_1, we calculated D_{mic} as a function of concentration. The result is displayed in Figure 1 as well. The increase of D_{mic} toward lower concentrations corresponds to a monotonic decrease of R_H, down to at least $R_H = 55$ Å at the lowest concentration investigated, which was about 5cmc.

2. Diffusion−Exchange Experiments on $C_{12}(EO)_5$/Latex/Water. The PFG experiment, as described above, was applied to samples with three different surfactant concentrations around and above full surface coverage with four different values of the gradient spacing, Δ, respectively. At lower concentrations the total surfactant signal was too low and at higher concentrations we found that the fast diffusing excess surfactant dominated the decay too strongly, so that no information about the bound surfactant site could be obtained. The echo decays for the intermediate concentrations are shown in Figures 2−4. In all data sets it is observed that the decay curve reflects the transition from slow to fast exchange with increasing Δ: The data have a double-exponential character for small Δ and become approximately monoexponential with increasing Δ.

To fit these data to the corresponding model functions, the following input parameters were used: The diffusion coefficient of the latex particles is calculated from the Stokes equation as $D_B = (2.1 \pm 0.1) \times 10^{-12}$ m^2/s. The value of T_1 is taken as $T_1 = 465 \pm 20$ ms and assumed to be independent of the aggregation state of the surfactant molecule, as determined from measurements of $C_{12}(EO)_5$ in water. For T_{2A} we chose the slowly relaxing component originating from the outer ethylene oxides to be the relevant one for the diffusion experiment,

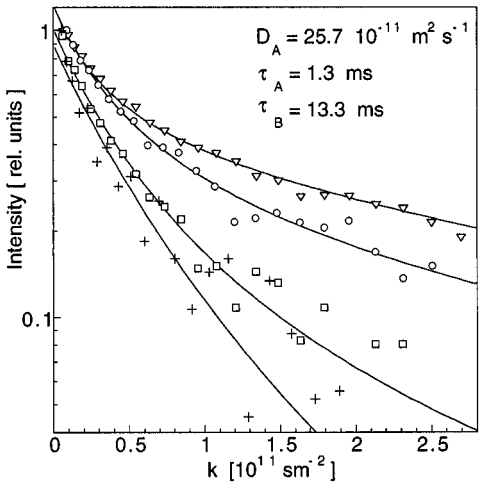

Figure 2. Echo decay curves of the PFG-stimulated echo sequence at total surfactant concentration $c = 0.698$ mg/mL: (▽) $\Delta = 15$ ms, (○) $\Delta = 25$ ms, (□) $\Delta = 50$ ms, (+) $\Delta = 100$ ms. The lines are the results of a global fit to all decay curves, yielding the parameters given in the figure.

TABLE 2: Results of the Monte-Carlo Error Analysis: Mean Values and Standard Deviation (in Parentheses) of the Resulting Fit Parameters τ_A, τ_B, and D_A. The Fraction of Adsorbed Surfactant f_B and the Area Per Molecule *A* Have Been Calculated from the Results of the Fit

c (mg/mL)	τ_A (ms)	τ_B (ms)	D_A (10^{-11} m^2 s^{-1})	f_B	A (Å^2)
0.698	1.4 (0.54)	13.4 (0.89)	28.1 (9.8)	0.909 (0.027)	56.4 (1.7)
0.905	3.2 (1.41)	9.3 (1.07)	14.8 (4.1)	0.757 (0.060)	53.2 (4.4)
1.22	7.1 (3.0)	7.0 (0.8)	9.9 (1.6)	0.518 (0.080)	58.3 (9.1)

neglecting the fast relaxation of the α-EO, since the latter has much lower intensity and is furthermore decaying faster. An average value of $T_{2A} = 340 \pm 40$ ms covers the relevant concentration range of the diffusion experiment. The determination of T_{2B}, even on very concentrated samples (20 vol % latex, in D_2O), caused some difficulties: The relaxation of adsorbed molecules is significantly enhanced due to their motions being restricted, leading to very low signal intensities that are moreover close to the water line at 4.7 ppm. Relaxation experiments on different samples and with different pulse sequences were not entirely consistent, the decay probably being two-exponential or more in nature, giving relaxation times in the range 3.6−6.6 ms. From the line width we obtained $T_{2B}^* \approx 4$ ms, although this value might be influenced by susceptibility effects originating from the latex surface. Different contributions to the Hahn echo might arise from different EO groups (see discussion of the binary system), the measurements might furthermore be affected by exchange, and T_{2B} might additionally vary with concentration. We therefore used $T_{2B} = 5$ ms with a large error interval of 2 ms to account for these variances.

In Figures 2−4 the fits of the diffusion data for different concentrations are displayed, together with the resulting parameters that were obtained as optimal fit with the original input data. Subsequently, Monte Carlo error analyses were performed. The results of the final parameters are given in Table 2. The numbers in parentheses are the standard deviations of the corresponding parameter. Covariances, that is interdependencies between pairs of the global parameters, were only found with respect to T_{2B}: D_A decreases and τ_A and τ_B increase with increasing T_{2B}. The errors of the other fixed parameters do not have a pronounced effect on the results.

The resulting values for the residence times are all in the range of several milliseconds and therefore considerably faster than adsorption rates obtained from nonequilibrium methods, where a surfactant depletion layer is limiting adsorption and determining the time scale. On the other hand, the resulting adsorption rates are much slower than the exchange between monomers and micelles, which can be described by the theory derived by Aniansson and co-workers.[19] The rate of monomers entering or leaving a micelle in equilibrium is given by the rate equation

$$k_+ \mathrm{cmc} = k_- N^{\mathrm{mic}} \tag{10}$$

where N^{mic} is the aggregation number, k_+ the monomer incorporation rate per micelle, and k_- the monomer desorption rate.

We will now estimate the exchange rates expected for diffusion-controlled exchange for the case of the colloidal system. Assuming that each monomer encountering the bead surface by diffusion is incorporated into the surface layer, the adsorption rate for monomers is given by $k_+^P = 4\pi R_B D_1$, where R_B is the latex particle radius and D_1 is the monomer diffusion coefficient. From the rate equation

$$k_+^{\mathrm{P}} \mathrm{cmc} = k_-^{\mathrm{P}} N^{\mathrm{P}} \tag{11}$$

with the index P referring to the latex particle and N^P being the number of surfactant molecules adsorbed per particle, the desorption rate k_-^P can be obtained. This desorption rate refers to a bound surfactant reaching a "free" state, where it is not subject to interaction with the surface, but rather undergoing free Gaussian diffusion with the diffusion coefficient D_A. Although this molecule might adsorb to the same surface again, resulting in a final displacement governed by D_B, its readsorption probability is controlled by k_+^P and the corresponding diffusion statistics, so that such a loop is still considered as a desorption−adsorption process. If, however, the molecule does not leave the range of interaction with the surface before returning, this process is rather governed by the interaction with the surface than by the diffusion statistics, so that during such a loop the molecule is considered as bound. This definition of free and bound states might cause inconsistencies at large particle concentrations, but is reasonable for dilute systems.

With N^P calculated from the molecular area of 56 Å^2 (see Table 2), the result is $\tau_B = 1/k_-^P = 12$ ms. This agrees well with the experimental value of $\tau_B = 13.4$ ms obtained from the measurement and fit at $c = 0.698$ mg/mL, indicating that at this concentration the equilibrium dynamics of adsorption are indeed mainly governed by the rate of diffusion of monomers onto the surface. This implies that the final monomer incorporation process into the layer does not limit the adsorption on the time scale of the experiment (10 ms). This is in agreement with experimental[4] and theoretical[7] findings of diffusion-controlled adsorption for nonionic surfactants at the air/liquid interface.

We note here that our result at this concentration corresponds to a situation where the free surfactant site consists mainly of monomers. With increasing concentration, τ_A is increasing, which reflects the increase of the surfactant concentration in site A. Simultaneously, τ_B is decreasing and does not correspond to the diffusion-limited value any more. Since the adsorption of monomers cannot occur faster than with the rate determined by the cmc and D_1 (see above), this increase in adsorption rate might be attributed to micelles that could take part in the exchange process as well. Assuming that a micelle can exchange monomers with the surface layer on collision with a bead, we can write the rate equation as

$$m\nu c^{\mathrm{mic}} + k_+^{\mathrm{P}} \mathrm{cmc} = k_-^{\mathrm{P}} N^{\mathrm{P}} \tag{12}$$

where m is the number of monomers adsorbed per collision and

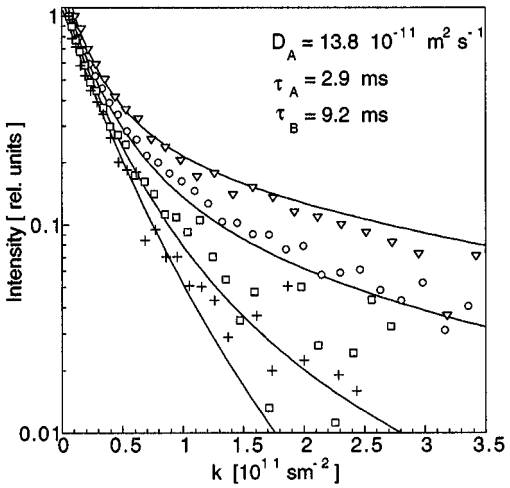

Figure 3. Echo decay curves of the PFG-stimulated echo sequence at total surfactant concentration $c = 0.905$ mg/mL: (▽) $\Delta = 15$ ms, (○) $\Delta = 25$ ms, (□): $\Delta = 50$ ms, (+) $\Delta = 100$ ms. The lines are the results of a global fit to all decay curves, yielding the parameters given in the figure.

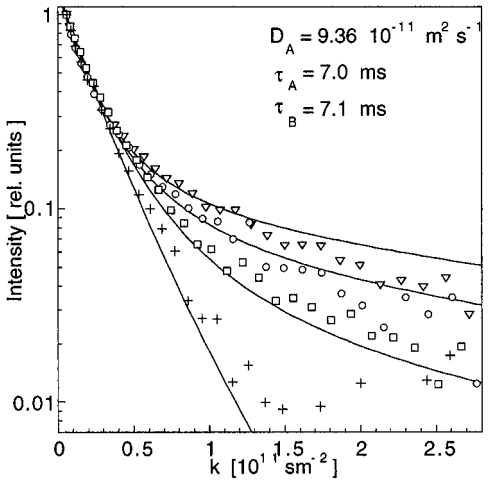

Figure 4. Echo decay curves of the PFG-stimulated echo sequence at total surfactant concentration $c = 1.22$ mg/mL: (▽) $\Delta = 10$ ms, (○) $\Delta = 25$ ms, (□): $\Delta = 50$ ms, (+) $\Delta = 100$ ms. The lines are the results of a global fit to all decay curves, yielding the parameters given in the figure.

TABLE 3: Comparison of f_B and A As Calculated from the Fit Results (Table 2) and with the Values Obtained from the Excess Concentration c_A Estimated from D_A

c (mg/mL)	c_A (D_A) (mg/mL)	f_B (D_A)	f_B (τ_A,τ_B)	A(D_A) (Å^2)	A(τ_A,τ_B) (Å^2)
0.698	0.035	0.949	0.909	54.0	56.4
0.905	0.088	0.903	0.757	44.3	53.2
1.22	0.149	0.878	0.518	33.6	58.3

$\nu = 4\pi D_{mic} R_B$ is the micelle-bead collision frequency. With the results of Table 2 for the higher concentrations and assuming small micelles with $R_{mic} = 20$ Å and $N_{mic} = 60$, a number of about 8 monomers that would have to be transferred per collision is obtained.

The fraction of adsorbed surfactant, $f_B = \tau_B/(\tau_A + \tau_B)$, and the resulting area per molecule, A, have been calculated and are given in Table 2. The molecular areas correspond roughly to the value obtained from ellipsometry data (45 Å^2 [20]), but are slightly larger. This might be due to the fact that the latex particles carry some electrical charges on the surface for electrostatic stabilization of the dispersion, which causes a reduced effective hydrophobic adsorption area. The area per molecule is not dependent on concentration, reflecting the fact that all three concentrations correspond to the plateau region with full surface coverage.

Another way of determining the surface coverage is to estimate the surfactant bulk concentration c_A from the dependence of the diffusion coefficient D_A on concentration that was measured for $C_{12}(EO)_5$ in H_2O. The data in Figure 1 were empirically described as $c_A(D_A) = 4.72 D_A^{-1.53}$. From this, $f_B(D_A)$ and $A(D_A)$ were calculated and compared to the values obtained directly from the residence times; see Table 3. We find good agreement for the lowest concentration; at higher concentration the adsorbed fraction is overestimated by this method. This is probably due to errors in the fit parameter D_A, which showed a strong correlation with the input parameter T_{2B}. Another possible explanation for the discrepancy of the molecular areas would be deviations from the two-site model. In fact, at higher surfactant concentrations the fits show small systematic deviations from the data at large k (see Figures 3 and 4), indicating that the two-site model assuming two well-defined diffusion coefficients does not perfectly describe the situation when a large micellar contribution is present. A reason for this might be polydispersity of the micelles or exchange between monomers and micelles. We have so far assumed monomer−micelle exchange to be fast compared to τ_A and τ_B, and this is confirmed by an estimate according to eq 10 for diffusion controlled micellar exchange, which results in $\tau = 1/k_- = 0.17$ ms for small spherical micelles. Furthermore the micellar exchange time scale has experimentally been found to be in the range of 0.1 ms for similar nonionic surfactants,[21] while for $C_{12}(EO)_5$ in an oil-in-water cubic phase, the residence time of surfactant molecules in an oil-swollen micelle was estimated to be 0.1 ms.[22] We therefore do not expect the exchange between the monomeric and micellar state to influence our results.

Conclusion

We have demonstrated that the method of exchange-coupled diffusion measured by PFG-NMR can be applied to surfactants adsorbed on solid surfaces to investigate the equilibrium dynamics of adsorption. The measurements of the nonionic surfactant $C_{12}(EO)_5$ on latex beads showed that at a concentration where the excess surfactant consists mainly of monomers the dynamics are governed by diffusion-limited adsorption of single monomers, whereas at higher concentrations an additional contribution of micellar surfactant to the exchange process was found.

As opposed to nonequilibrium measurements of adsorption dynamics, measurements are possible on a faster time scale with this equilibrium method, since the diffusion limit is faster in equilibrium. Furthermore, it gives the opportunity for studying adsorption dynamics at solid interfaces. This makes PFG-NMR despite the low sensitivity in the NMR experiments and the necessity of a thorough numerical analysis of the raw data an interesting tool to further investigate adsorption dynamics. This holds especially for cases where the dynamics are not governed by diffusion, but additionally slowed due to kinetic effects such as energetic barriers in the final incorporation process of a monomer into the surface layer, such as electrostatic repulsion in the case of ionic surfactants.

Acknowledgment. This work has been supported by the European Commission, program TMR, contract no. ERBFMBICT961178, and by the Swedish National Science Research Council. The spectrometer used was financed by a grant from the Swedish Planning and Coordination of Research.

References and Notes

(1) Chang, C.-H.; Franses, E. I. *Colloids Surf. A* **1995**, *100*, 1.
(2) Ward, A. F. H.; Tordai, L. *J. Chem. Phys.* **1946**, *14*, 453.
(3) Borwankar, R. P.; Wasan, D. T. *Chem. Eng. Sci.* **1983**, *38*, 1637.
(4) Fainerman, V. B.; Miller, R. *J. Colloid Interface Sci.* **1996**, *178*, 168.
(5) Tiberg, F.; Jönsson, B.; Lindman, B. *Langmuir* **1994**, *10*, 3714.
(6) Lin, S.-Y.; McKeigue, K.; Maldarelli, C. *Langmuir* **1994**, *10*, 3442.
(7) Diamant, H.; Andelman, D. *J. Phys. Chem.* **1996**, *100*, 13732.
(8) Stejskal, E. O.; Tanner, J. E. *J. Chem. Phys.* **1965**, *42*, 288.
(9) Stilbs, P. *Prog. Nucl. Magn. Reson. Spectrosc.* **1987**, *19*, 1.
(10) Callaghan, P. T. *Principles of Nuclear Magnetic Resonance Microscopy*; Clarendon Press: Oxford, 1991.
(11) Kärger, J. *Ann. Phys.* **1971**, *7* (27), 107.
(12) Alper, J. S.; Gelb, R. I. *J. Phys. Chem.* **1990**, *94*, 4747.
(13) Olofsson, G. *J. Phys. Chem.* **1985**, *89*, 1473.
(14) Nilsson, P. G.; Wennerström, H.; Lindman, B. *J. Phys. Chem.* **1983**, *87*, 1377.
(15) Jonströmer, M.; Jönsson, B.; Lindman, B. *J. Phys. Chem.* **1991**, *95*, 3293.
(16) Brown, W.; Pu, Z.; Rymden, R. *J. Phys. Chem.* **1988**, *92*, 6086.
(17) Thuresson, K.; Söderman, O.; Hansson, P.; Wang, G. *J. Phys. Chem.* **1996**, *100*, 4909.
(18) Kamenka, N.; Puyal, M.; Brun, B.; Haouche, G.; Lindman, B. In *Surfactants in Solution*; Mittal, K. L., Lindman, B., Eds.; Plenum: New York, 1984; Vol. 1, p 359.
(19) Aniansson, E. A. G.; Wall, S. N.; Almgren, M.; Hoffmann, H.; Kielmann, W.; Ulbricht, W.; Zana, R.; Lang, J.; Tondre, C. *J. Phys. Chem.* **1976**, *80*, 905.
(20) Tiberg, F.; Jönsson, B.; Tang, J.-a.; Lindman, B. *Langmuir* **1994**, *10*, 2294.
(21) Alami, E.; van Os, N. M.; Rupert, L. A. M.; de Jong, B.; Kerkhof, F. J. M.; Zana, R. *J. Colloid Interface Sci.* **1993**, *160*, 205.
(22) Rajagopalan, V.; Leaver, M.; Mortensen, K.; Olsson, U. Manuscript in preparation.